SAND2020-10892C

# Solving inverse problems for process-structure linkages using asynchronous parallel Bayesian optimization *

Anh Tran, Tim Wildey

**Abstract** Process-structure linkage is one of the most important topics in materials science due to the fact that virtually all information related to the materials, including manufacturing processes, lies in the microstructure itself. Therefore, to learn more about the process, one must start by thoroughly examining the microstructure. This gives rise to inverse problems in the context of process-structure linkages, which attempt to identify the processes that were used to manufacturing the given microstructure. In this work, we present an inverse problem for structure-process linkages which we solve using asynchronous parallel Bayesian optimization which exploits parallel computing resources. We demonstrate the effectiveness of the method using kinetic Monte Carlo model for grain growth simulation.

## 1 Introduction

Process-structure-property linkages are the hallmarks of materials science, to which numerous efforts in experiments, theoretical models, computational simulations, and machine learning have been made to establish the relationship [8]. Since the Materials Genome Initiative [20] has been introduced to reduce the development time for new materials, machine learning has emerged as one of the most potential solutions to reduce experimental and computational efforts. Many integrated computational materials engineering (ICME) models and simulations [4, 19, 14] have been introduced and developed to simulate experiments as forward prediction computational toolboxes, the materials design should be addressed from the inverse problem perspective [21, 1, 13]. In this regard, microstructure is often bypassed, and the process-structure-property is then shortened to process-property linkage by ignoring the materials microstructure. However, it is often considered that microstructure is the great source of information, containing most, if not all, process-related information. Here, we applied our previous framework in solving inverse problem of structure-process linkages using asynchronous parallel Bayesian optimization (BO) on high-performance computing (HPC) platform. The problem statement can be succinctly described as follows. Given a microstructure and a predictive ICME model which allows simulations of the process-structure linkage, determine the process(es) and the associated processing parameters that were used to produce the given microstructure. We also assume that the manufacturing processes are parameterizable using continuous, discrete, and random variables.

Anh Tran, Tim Wildey
Center for Computing Research
Optimization and Uncertainty Quantification Department
Sandia National Laboratories
e-mail: anhtran@sandia.gov

* This research was supported by the U.S. Department of Energy, Office of Science, Early Career Research Program.

Numerous studies have been conducted to optimize one or multiple materials properties, which are directly related to materials performance. Typical approaches often treat materials properties as scalar outputs, where manufacturing processes can be parameterized by either discrete or continuous variables. Recent advanced studies also include random variables to incorporate uncertainty quantification (UQ). Most commonly used methods are bio-inspired heuristic optimization methods, such as genetic algorithms, particle swarm optimization algorithms, and surrogate-based optimization methods, such as Bayesian optimization algorithms [31, 32], which is based on Gaussian process regression (GPR). In our previous work [27], we proposed asynchronous parallel BO, which is adopted to solve the grain growth problem in this paper.

While BO has been extensively used in literature, our approach [26] significantly leverages the computational effort in minimizing the wall-clock time deployment for computationally expensive simulations, by smartly submitting and retrieving results in an asynchronous manner, where the number of simulations queried is user-defined. For those with large computational resources, this framework allows one to run more simulations with different inputs and converge quicker with at least a factor of $\sqrt{B}$ speedup, where $B$ is the batch size. In this BO framework, the single-objective is scalarized from multiple objectives, where each objective measures the deterministic or statistical difference between the candidate and target microstructures. To measure the difference, we employ a number of microstructure descriptors, where the majority are statistical microstructure descriptors, such as grain size distribution, chord-length distribution, etc. The objective function can be regarded as the statistical metrics between two probability density functions (pdfs) of the same microstructure descriptors, applied on the target and candidate microstructures, respectively.

## 2 Methodology

In the context of process-structure-property linkages in materials science, process is usually referred to manufacturing process(es) and is often characterized by an exhaustive description to elaborate the procedure to produce a specific material, which in turns can be parameterized using continuous and discrete variables. In this regard, it is conventional to treat manufacturing process as deterministic variables, as they exhibit some sort of controllable behaviors that can use to reproduce the same materials. Structure, which is usually referred to microstructures, which is well-known to exhibit inherent randomness, for example, spatial variation on the same specimen. As such, it is conventional to characterize microstructure using an exhaustive set of microstructure descriptors to rigorously quantify the bound of these random behaviors. To this end, it is reasonable to treat microstructure descriptors as either deterministic or statistical variables.

### 2.1 Problem formulation

In the asynchronous parallel BO workflow for process-structure linkage, the inputs are the parameterized processing parameters, and the output is the scalarized single-objective in solving the multi-objective optimization problem. For each proposed candidate microstructure, which is the output of the predictive ICME model coupling process-structure linkage that corresponds to the proposed input parameter, we applied the conditional microstructure descriptors on the target and candidate microstructures, respectively, to produce a set of probability density functions (pdfs) of conditional microstructure descriptors. We then use statistical functions to numerically measure the difference between two pdfs, which represents an objective in the multi-objective optimization problem. Multiple objectives can then be scalarized using the augmented Tchebycheff function. Each of the following subsections describes a key component of this BO workflow.

## 2.2 Materials characterization by microstructure descriptors

Microstructure are inherently random, varying spatially from one location to another on the same specimen. The usage of microstructure descriptors on a sufficiently large microstructure to reduce bias is a well-known technique for computational characterization of microstructure. There are two types of microstructure descriptors: deterministic and statistical. Deterministic microstructure descriptors includes, but are not limited to, volume fraction, total surface area, number of cluster, number of grains, etc. Statistical microstructure descriptors are more commonly used and represented in the form of probability density function, which includes, but are not limited to, equivalent radius distribution, compactness distribution, aspect ratio distribution, etc.

To compare between two microstructures quantitatively and measure how far they are away from each, one needs to impose many microstructure descriptors, including both statistical and deterministic. The microstructure descriptors must be able to distinguish one microstructure from another, quantitatively. Because of the stochastic nature of microstructure, the statistical microstructure descriptors are used more often than the deterministic ones. Suppose that there are $s$ microstructure descriptors, denoted as $\{d_i\}_{i=1}^{s}$. Given a microstructure, one can collect a population of grains, and subsequently build a statistics on the grain population with a probability density function representation. For example, one can (i) compute the grain area for each grain in the microstructure, (ii) collect all the observations, and (iii) approximate the probability density function of the observational grain areas of the microstructure.

## 2.3 Measures of differences between microstructures via microstructure descriptors

While both deterministic and statistical microstructure descriptors are very useful in characterize materials, they could be numerically ill-conditioned. In other words, to compare microstructures, one may impose other conditions to highlight the difference between target and candidate microstructures. If applied, such conditions would leverage the typical microstructure descriptors to the conditional microstructure descriptors, which only compare the difference between two microstructures if the condition is satisfied. For example, if the dominant grain population is very small, one may need to ignore the small grain population and compare only the larger grain population, which can be easily applied by thresholding. Such problems are fairly common in practice, such as in additive manufacturing via powder bed fusion.

If the microstructure descriptor is statistical and can be represented as a probability density function, some statistical metrics and divergences, for example, Wasserstein distance and Kullback-Leibler divergence, can be utilized to measure the difference between probability density functions. A list of statistical metrics is briefly discussed in [3, 17, 6]. We note that using statistical moments to characterize a probability density function is a poor approach due to numerically ill-conditioned of moments [10]. In particular, if the Kullback-Leibler divergence is utilized to measure the statistical difference $\mathcal{S}(\cdot)$, then the statistical difference between microstructures for a specific microstructure is computed as

$$\begin{aligned} S\Big(p_D(d|\mathbf{candidateMs}),\ p_D(d|\mathbf{targetMs})\Big) &= \mathrm{KL}\Big(p_D(d|\mathbf{targetMs})\ \|\ p_D(d|\mathbf{candidateMs}\Big) \\ &= \int p_D(d|\mathbf{targetMs})\ \log\left(\frac{p_D(d|\mathbf{targetMs})}{p_D(d|\mathbf{candidateMs})}\right)\partial d \qquad , \end{aligned} \tag{1}$$

where $\mathrm{KL}(\cdot)$ denotes the Kullback-Leibler divergence and $d$ is the microstructure descriptor.

## 2.4 Objective functions

The differences between these microstructure descriptors are then considered as the objective functions, i.e. $y_i = \mathcal{S}_i\Big(p_{D_i}(d_i|\textbf{targetMs}),\ p_{D_i}(d_i|\textbf{candidateMs})\Big),\ i = 1, \ldots, s$ where the goal is to minimize $s$ objectives, $\{y_i\}_{i=1}^{s}$, simultaneously. It is noteworthy that these objective functions are typically noisy due to the fact that the microstructure considered is within finite domain, thus bias can be reduced but cannot be eliminated. As a result, one can regard that our framework [27] formulates the inverse problems in structure-property as a multi-objective optimization problem, where BO is used.

## 2.5 Asynchronous parallel Bayesian optimization framework

In our previous work, we have extended the traditional Bayesian optimization framework into synchronously batch-sequential parallel Bayesian optimization [28] for constrained optimization problems, called pBO-2GP-3B, where the constraints are generalized to cover a broad spectrum of applications by considering both known and unknown constraints. We deployed a further improved implementation of pBO-2GP-3B, called aphBO-2GP-3B [26], to asynchronously parallelize on the high-performance computing environment with multiple acquisition functions considered. A brief description of BO is provided in the remainder of this section. Interested readers are further referred to our BO previous work [29, 30, 25].

Assume that $f$ is a function of $\boldsymbol{x}$, where $\boldsymbol{x} \in \mathcal{X}$ is a $d$-dimensional input, and $y$ is the observation. Let the dataset $\mathcal{D} = (\boldsymbol{x}_i, y_i)_{i=1}^{n}$, where $n$ is the number of observations. A GP regression assumes that $\boldsymbol{f} = f_{1:n}$ is jointly Gaussian, and the observation $y$ is normally distributed given $f$,

$$\boldsymbol{f}|\boldsymbol{X} \sim \mathcal{N}(\boldsymbol{m}, \boldsymbol{K}), \quad \boldsymbol{y}|\boldsymbol{f}, \sigma^2 \sim \mathcal{N}(\boldsymbol{f}, \sigma^2\boldsymbol{I}), \tag{2}$$

where $m_i := \mu(\boldsymbol{x}_i)$ and $K_{i,j} := k(\boldsymbol{x}_i, \boldsymbol{x}_j)$. The covariance kernel $\boldsymbol{K}$ is a choice of modeling covariance between inputs. At an unknown sampling location $\boldsymbol{x}$, the predicted response is described by a posterior Gaussian distribution, where the posterior mean is

$$\mu_n(\boldsymbol{x}) = \mu_0(\boldsymbol{x}) + \boldsymbol{k}(\boldsymbol{x})^T(\boldsymbol{K} + \sigma^2\boldsymbol{I})^{-1}(\boldsymbol{y} - \boldsymbol{m}), \tag{3}$$

and the posterior variance is

$$\sigma_n^2 = k(\boldsymbol{x}, x) - \boldsymbol{k}(\boldsymbol{x})^T(\boldsymbol{K} + \sigma^2\boldsymbol{I})^{-1}\boldsymbol{k}(\boldsymbol{x}), \tag{4}$$

where $k(\boldsymbol{x})$ is the covariance vector between the query point $\boldsymbol{x}$ and $\boldsymbol{x}_{1:n}$. The classical GP formulation assumes stationary covariance matrix, which only depends on the distance $r = \|\boldsymbol{x} - \boldsymbol{x}'\|$. While numerous kernels have been used in the literature, we focus on squared exponential kernel in this work. Optimizing the log-likelihood function yields the hyper-parameter $\theta$ at the computational cost of $\mathcal{O}(n^3)$ due to the cost to compute the inverse of the covariance matrix.

The acquisition function for probability of improvement (PI) [9] is defined as

$$a_{\text{PI}}(\boldsymbol{x}; \{\boldsymbol{x}_i, y_i\}_{i=1}^{N}, \theta) = \Phi(\gamma(\boldsymbol{x})), \tag{5}$$

where $\gamma(\boldsymbol{x})$ indicates the deviation away from the best sample. The acquisition function for expected improvement (EI) scheme [11, 12, 2, 22] is defined as

$$a_{\text{EI}}(\boldsymbol{x}; \{\boldsymbol{x}_i, y_i\}_{i=1}^{N}, \theta) = \sigma(\boldsymbol{x}; \{\boldsymbol{x}_i, y_i\}_{i=1}^{N}, \theta) \cdot (\gamma(\boldsymbol{x})\Phi(\gamma(\boldsymbol{x})) + \phi(\gamma(\boldsymbol{x})) \tag{6}$$

The acquisition function for the upper-confidence bounds (UCB) scheme [23, 24] is defined as

$$a_{\mathrm{UCB}}(\boldsymbol{x}; \{\boldsymbol{x}_i, y_i\}_{i=1}^N, \theta) = \mu(\boldsymbol{x}; \{\boldsymbol{x}_i, y_i\}_{i=1}^N, \theta) + \kappa\sigma(\boldsymbol{x}; \{\boldsymbol{x}_i, y_i\}_{i=1}^N, \theta), \tag{7}$$

where $\kappa$ is a hyper-parameter describing the acquisition exploitation-exploration balance.

Multi-objective optimization problems are typically solved by converting a multi-objective problem to a single-objective problem, where the single objective is a weighted sum of multiple objectives [18]. While there is no restriction on the optimization method that can be used to minimize the difference between the candidate and the target microstructures, in this work, we use the aphBO-2GP-3B BO framework, which is an asynchronously parallel constrained multi-acquisition BO algorithm to further improve its efficiency on HPC platforms. The aphBO-2GP-3B subdivides the computational budget into three batches, supported by two GPRs. One GPR is used to model the objective function, whereas another GPR is used as a probabilistic binary classifier for hidden constraints. The first batch focuses on optimizing the objective functions by sampling at the locations where the acquisition function value of the Bayesian optimization is maximized. The second batch focuses on the exploration, by sampling at the locations where the posterior variance is maximized. The third batch focuses on the feasibility classification to learn hidden constraints from the optimization problem. The acquisition function is sampled with probabilities exponentially scaled with rewards, in the same manner with GP-Hedge algorithm [7].

## 3 Case study: kinetic Monte Carlo simulation

In this section, we demonstrate the applicability of asynchronous parallel BO in solving the inverse problem in process-structure linkages using kinetic Monte Carlo with numerical temperatures. Similar to the second case studies in our previous work [27], in this example, we set a different numerical temperature with $k_B T_s = 0.85$.

### 3.1 Kinetic Monte Carlo simulation

The details of temperature-dependent kMC simulation for grain growth and its implementation in Sandia/SPPARKS [15, 16] is described in Garcia et al [5], and is summarized here for the sake of completeness. In the grain growth simulation, the Potts model [33] is used to simulate curvature-driven grain growth. The Arrhenius equation describes the relationship between grain boundary mobility and temperature and the Metropolis algorithm is used to determine the probability of successful change in grain site orientation as

$$P = \begin{cases} \exp\left(\dfrac{-\Delta E}{k_B T_s}\right), & \text{if } \Delta E > 0, \\ 1, & \text{if } \Delta E \leq 0, \end{cases} \tag{8}$$

where $E$ is the total grain boundary energy calculated by summing all the neighbor interaction energies, $\Delta E$ can be regarded as the activation, and $T_s$ is the simulation temperature.

### 3.2 Statistical microstructure descriptors as outputs

Figure 1a shows the effect of $k_B T_s$ on different grain growth microstructure. In particular, larger $k_B T_s$ is associated with microstructures with smaller grain size for (nearly) the same amount of time. This suggests that the grain size distribution may be a good microstructure descriptor to describe and distinguish one microstructure from another.

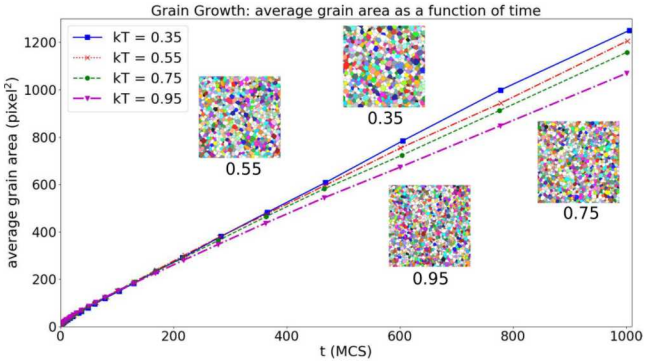


(a) Effects of the numerical temperature $k_B T_s$ in the kMC grain growth problem. Reprinted with permission from [27].

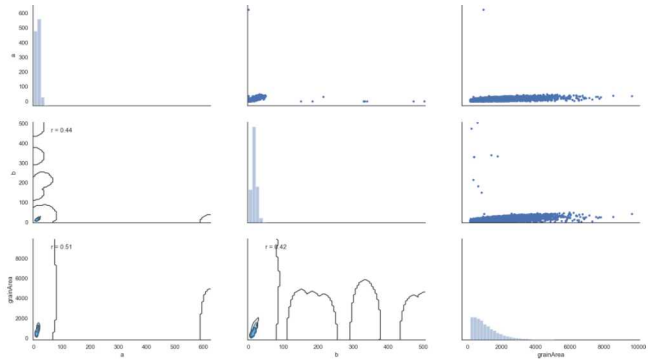

(b) Pair plot between microstructure descriptors: major dimensions of best-fit ellipse, minor dimensions of best-fit ellipse, and grain area.

Fig. 1: Grain growth and its dependence on temperature (Figure 1a). Statistical microstructure descriptors and their pairwise correlations (Figure 1b).

In this case study, the distribution of grain area is used as the microstructure descriptor, where the Kullback-Leibler divergence measuring the difference between candidate and target microstructures is used as an output, where $k_B T_s$ is the numerical input describing simulation temperature. Because the number of grains are fairly small (few thousands), no filter is imposed on the statistical microstructure descriptors. In the target microstructure, $k_B T_s$ is set as 0.70, where the range of candidate microstructures is $[0.25, 0.95]$. The size of the simulation domain is 1024×1024, which takes about 300s with 18 processors ($\approx$ 1.5 CPU hours).

### 3.3 Numerical results

In this example, $k_B T_s$ is set at 0.85. A computational domain of 1024 pixel × 1024 pixel is used to set up the numerical experiment. For consistency, all calculations are performed on Sandia's *Blake* cluster consisting of dual-socket Intel(R) Xeon(R) (Platinum) 8160 CPU with 24 cores per node.The upper and lower bounds of objectives for three optimization runs are plotted as blue envelope in Figure 2a. Two sampling points at $k_B T_s \in \{0.25, 0.95\}$ are initialized. Here, one iteration corresponds to a single kMC simulation with different parameters. The single-objective $y$ starts at 0.27194599 for iteration 0, 0.01099406 for iteration 1, and 0.00322190 for iteration 12. The optimal input parameter $k_B T_s$ is 0.85720249, which agrees very well with the target input parameter $k_B T_s$ of 0.85. Figure 2b presents the state of specific workers, i.e. whether they are idle (green) or busy (blue, pink, yellow, or orange), which we refer to as the schedule. Furthermore, one can see what acquisition is being queried at specific time with the schedule. The optimization run ends when workers finish their last job.

## 4 Conclusions

In this paper, we applied our previous framework [27] to solve the inverse problem in process-structure linkages, where microstructure descriptors are used to characterize the microstructure on-the-fly. Statistical divergence, i.e. Kullback-Leibler divergence is then applied to measure the differences between candidate and target microstructure,

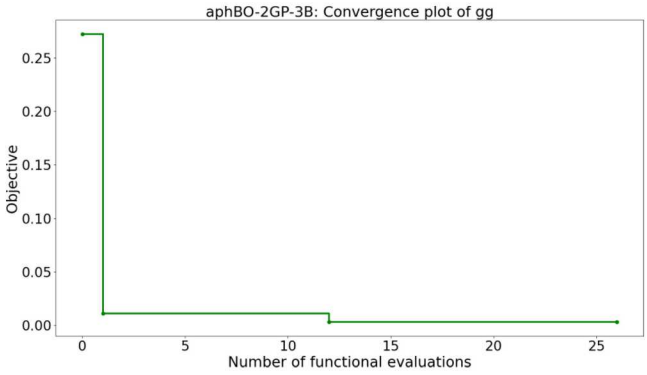


(a) Convergence plot of the microstructure calibration framework in kMC/grain growth problem.

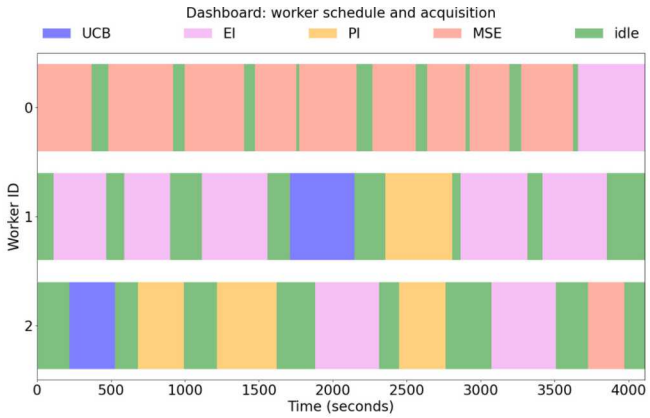


(b) Scheduler for asynchronous parallel Bayesian optimization.

Fig. 2: Convergence plot (Figure 2a) and scheduler (Figure 2b) for the asynchronous parallel aphBO-2GP-3B [26] framework. Readers are referred to online color version.

respectively. To that end, an asynchronous parallel BO framework is applied to minimize their numerical differences. We demonstrate its application using kinetic Monte Carlo examples, where the numerical temperature is successfully recovered for our case study.

## Acknowledgment

The views expressed in the article do not necessarily represent the views of the U.S. Department of Energy or the United States Government. Sandia National Laboratories is a multimission laboratory managed and operated by National Technology and Engineering Solutions of Sandia, LLC., a wholly owned subsidiary of Honeywell International, Inc., for the U.S. Department of Energy's National Nuclear Security Administration under contract DE-NA-0003525. This research was supported by the U.S. Department of Energy, Office of Science, Early Career Research Program.

## References

1. Arróyave, R., McDowell, D.L.: Systems approaches to materials design: Past, present, and future. Annual Review of Materials Research **49**(1), 103–126 (2019)
2. Bull, A.D.: Convergence rates of efficient global optimization algorithms. Journal of Machine Learning Research **12**(Oct), 2879–2904 (2011)
3. Cha, S.H.: Comprehensive survey on distance/similarity measures between probability density functions. City **1**(2), 1 (2007)
4. Chaparro, B., Thuillier, S., Menezes, L., Manach, P.Y., Fernandes, J.: Material parameters identification: Gradient-based, genetic and hybrid optimization algorithms. Computational Materials Science **44**(2), 339–346 (2008)
5. Garcia, A.L., Tikare, V., Holm, E.A.: Three-dimensional simulation of grain growth in a thermal gradient with non-uniform grain boundary mobility. Scripta Materialia **59**(6), 661–664 (2008)
6. Gibbs, A.L., Su, F.E.: On choosing and bounding probability metrics. International statistical review **70**(3), 419–435 (2002)
7. Hoffman, M., Brochu, E., de Freitas, N.: Portfolio allocation for bayesian optimization. In: Proceedings of the Twenty-Seventh Conference on Uncertainty in Artificial Intelligence, UAI'11, pp. 327–336. AUAI Press, Arlington, Virginia, USA (2011)
8. Kalidindi, S.R., Medford, A.J., McDowell, D.L.: Vision for data and informatics in the future materials innovation ecosystem. JOM **68**(8), 2126–2137 (2016)

9. Kushner, H.J.: A new method of locating the maximum point of an arbitrary multipeak curve in the presence of noise. Journal of Basic Engineering **86**(1), 97–106 (1964)
10. Mnatsakanov, R.M.: Hausdorff moment problem: Reconstruction of probability density functions. Statistics & probability letters **78**(13), 1869–1877 (2008)
11. Mockus, J.: On Bayesian methods for seeking the extremum. In: Optimization Techniques IFIP Technical Conference, pp. 400–404. Springer (1975)
12. Mockus, J.: The Bayesian approach to global optimization. System Modeling and Optimization pp. 473–481 (1982)
13. Olson, G.: Genomic materials design: the ferrous frontier. Acta Materialia **61**(3), 771–781 (2013)
14. Ong, S.P.: Accelerating materials science with high-throughput computations and machine learning. Computational Materials Science **161**, 143–150 (2019)
15. Plimpton, S., Battaile, C., Chandross, M., Holm, L., Thompson, A., Tikare, V., Wagner, G., Webb, E., Zhou, X., Cardona, C.G., et al.: Crossing the mesoscale no-man's land via parallel kinetic Monte Carlo. Sandia Report SAND2009-6226 (2009)
16. Plimpton, S., Thompson, A., Slepoy, A.: SPPARKS kinetic monte carlo simulator (2012)
17. Rachev, S.T., Klebanov, L.B., Stoyanov, S.V., Fabozzi, F.J.: Probability distances and probability metrics: definitions. In: The Methods of Distances in the Theory of Probability and Statistics, pp. 11–31. Springer (2013)
18. Rojas-Gonzalez, S., Van Nieuwenhuyse, I.: A survey on kriging-based infill algorithms for multi-objective simulation optimization. FEB Research Report KBI_1907 (2019)
19. Salzbrenner, B.C., Rodelas, J.M., Madison, J.D., Jared, B.H., Swiler, L.P., Shen, Y.L., Boyce, B.L.: High-throughput stochastic tensile performance of additively manufactured stainless steel. Journal of Materials Processing Technology **241**, 1–12 (2017)
20. Science, N., (US), T.C.: Materials Genome Initiative for global competitiveness. Executive Office of the President, National Science and Technology Council (2011)
21. Sinnott, S.B.: Material design and discovery with computational materials science. Journal of Vacuum Science & Technology A: Vacuum, Surfaces, and Films **31**(5), 050812 (2013)
22. Snoek, J., Larochelle, H., Adams, R.P.: Practical Bayesian optimization of machine learning algorithms. In: Advances in Neural Information Processing Systems, pp. 2951–2959 (2012)
23. Srinivas, N., Krause, A., Kakade, S.M., Seeger, M.: Gaussian process optimization in the bandit setting: No regret and experimental design. arXiv preprint arXiv:0912.3995 (2009)
24. Srinivas, N., Krause, A., Kakade, S.M., Seeger, M.W.: Information-theoretic regret bounds for Gaussian process optimization in the bandit setting. IEEE Transactions on Information Theory **58**(5), 3250–3265 (2012)
25. Tran, A., Eldred, M., Wang, Y., McCann, S.: srMO-BO-3GP: A sequential regularized multi-objective constrained Bayesian optimization for design applications. In: Proceedings of the ASME 2020 IDETC/CIE, *International Design Engineering Technical Conferences and Computers and Information in Engineering Conference*, vol. Volume 1: 40th Computers and Information in Engineering Conference. American Society of Mechanical Engineers (2020)
26. Tran, A., McCann, S., Furlan, J.M., Pagalthivarthi, K.V., Visintainer, R.J., Wildey, T., Eldred, M.: aphBO-2GP-3B: A budgeted asynchronous-parallel multi-acquisition for known/unknown constrained Bayesian optimization on high-performing computing architecture. arXiv preprint arXiv:2003.09436 (2020)
27. Tran, A., Mitchell, J.A., Swiler, L.P., Wildey, T.: An active-learning high-throughput microstructure calibration framework for process-structure linkage in materials informatics. Acta Materialia **194**, 80–92 (2020)
28. Tran, A., Sun, J., Furlan, J.M., Pagalthivarthi, K.V., Visintainer, R.J., Wang, Y.: pBO-2GP-3B: A batch parallel known/unknown constrained Bayesian optimization with feasibility classification and its applications in computational fluid dynamics. Computer Methods in Applied Mechanics and Engineering **347**, 827–852 (2019)
29. Tran, A., Tran, M., Wang, Y.: Constrained mixed-integer Gaussian mixture Bayesian optimization and its applications in designing fractal and auxetic metamaterials. Structural and Multidisciplinary Optimization pp. 1–24 (2019)
30. Tran, A., Tranchida, J., Wildey, T., Thompson, A.P.: Multi-fidelity machine-learning with uncertainty quantification and Bayesian optimization for materials design: Application to ternary random alloys. The Journal of Chemical Physics **153**, 074705 (2020)
31. Tran, A., Wildey, T., McCann, S.: sBF-BO-2CoGP: A sequential bi-fidelity constrained Bayesian optimization for design applications. In: Proceedings of the ASME 2019 IDETC/CIE, *International Design Engineering Technical Conferences and Computers and Information in Engineering Conference*, vol. Volume 1: 39th Computers and Information in Engineering Conference. American Society of Mechanical Engineers (2019). V001T02A073
32. Tran, A., Wildey, T., McCann, S.: sMF-BO-2CoGP: A sequential multi-fidelity constrained Bayesian optimization for design applications. Journal of Computing and Information Science in Engineering **20**(3), 1–15 (2020)
33. Wu, F.Y.: The Potts model. Reviews of modern physics **54**(1), 235 (1982)